

Turbidity determination of the critical exponent η in the liquid–liquid mixture methanol and cyclohexane

Amy Lytle and D. T. Jacobs^{a)}

Physics Department, The College of Wooster, Wooster, Ohio 44691

(Received 17 November 2003; accepted 16 December 2003)

The turbidity of the liquid–liquid mixture methanol–cyclohexane has been measured very near its critical point and used to test competing theoretical predictions and to determine the critical correlation-correction exponent η . By measuring the ratio of the transmitted to incident light intensities over five decades in reduced temperature, we are able to determine that Ferrell's theoretical prediction for the turbidity explains the data with the correlation length amplitude $\xi_0 = 0.330 \pm 0.003$ nm and critical exponents $\eta = 0.041 \pm 0.005$ and $\nu = 0.632 \pm 0.002$. These values are consistent with the values measured before for ξ_0 in this system and with the exponents predicted by theory. The data allow five different theoretical expressions to be tested and to select two as being equivalent when very close to the critical point. © 2004 American Institute of Physics.

[DOI: 10.1063/1.1647524]

I. INTRODUCTION

The turbidity measures the amount of light that can be transmitted through a fluid, but in the process also determines much about the concentration fluctuations that dominate a system's behavior near its critical point. Large density or concentration fluctuations involve many length scales that effectively mask the identity of the system and produce universal phenomena. Many physical quantities behave as a simple power law when a system is near its critical point and is explored along various thermodynamic paths. For example, the correlation length ξ diverges close to the critical point as a power law $\xi = \xi_0 t^{-\nu}$, where $t \equiv (T - T_c)/T_c$ is the reduced temperature, ξ_0 is a system-dependent amplitude, and ν is the critical exponent. The critical exponents describing these relationships are universal and should depend only on a universality class determined by the order parameter and spatial dimensionality of the system. Liquid–gas, liquid–liquid mixtures, uniaxial ferromagnetism, polymer–solvent, and ionic solutions are all thought to belong to the same universality class: the three-dimensional Ising model.¹

The development in 1971 of renormalization group theory from earlier concepts of scaling and universality provided a theoretical framework for distinguishing systems, predicting critical exponent relations, approximating values for critical exponents, and obtaining amplitude relations. Several universal exponents have been predicted using various numerical techniques,² which now provide consistent prediction^{3–5} (see Table I), most of which have been confirmed by experiments. Turbidity is often used to determine exponents and amplitudes in simple liquid–gas or liquid–liquid systems as well as in complex systems such as a plastic crystal in water,⁶ a polymer in a weak solvent,^{7,8} or ionic systems.⁹ A particularly powerful observation is that only two critical exponents are linearly independent with others

determined by scaling relations [i.e., $\gamma = (2 - \eta)\nu$], and that the leading amplitudes are interrelated using only two scale factors. Thus, in principle the universality of the exponents could be used with two experiments to determine all the leading critical behavior of a given system.

A liquid–liquid mixture exhibiting an upper consolute point will be one phase, homogeneous, and essentially clear when the mixture is well above its critical consolute temperature T_c . As the temperature of the fluids approaches T_c , concentration fluctuations cause the transmitted light intensity I to be reduced from the incident intensity I_0 . The total incremental intensity of light scattered per unit length is defined as the turbidity τ

$$\tau = L^{-1} \ln(I_0/I), \quad (1)$$

where L is the optical path length.

Previous experiments had yet to convincingly verify the theoretical prediction for the critical correlation-correction (or Green–Fisher) exponent η , which would be an important confirmation¹⁰ of the fundamental physics that underpins the theoretical framework for critical-point phenomena. Three principal techniques have been used to look for η , and they all involve scattering phenomena using either x rays, neutrons, or light. To determine η , the experiment must reach large values of $k\xi$, where k is the scattering vector, which varies as the reciprocal of the wavelength λ , and ξ is the correlation length. X rays and neutrons can achieve large values of k , but those experiments have difficulty getting close to the critical point (large ξ). Moreover, the wavelength of the incident radiation must be long compared to the range of the interatomic forces, which is difficult to do in present x-ray and neutron scattering experiments. Light scattering, on the other hand, has relatively long wavelengths (smaller k values) and must resort to a very close approach to the critical point (large ξ). If light intensity is measured as a function of angle, then a close approach to the critical point is precisely where the problem of multiple scattering is most pro-

^{a)}Author to whom correspondence should be addressed. Electronic mail: djacobs@wooster.edu

TABLE I. Theoretical values of the critical exponents, which use the scaling relation $\gamma=(2-\eta)\nu$.

γ	ν	η	Ref. no.
1.2373±0.0002	0.63012±0.000 16	0.036 39±0.000 15	3
1.2355±0.0050	0.6290±0.002 5	0.036 0±0.005 0	4
1.2396±0.0013	0.6304±0.001 3	0.033 5±0.002 5	4
1.2395	0.6320	0.038 8	5

nounced. However, multiple scattering has little effect on turbidity measurements, which makes them attractive to determine the exponent η .

In an earlier paper,¹¹ we reported preliminary turbidity data and how that can determine the exponent η from a theoretical prediction by Ferrell, and we also summarized the experimental determinations for the exponent η in Ising systems. There are two additional neutron scattering experiments: one in a liquid–gas system¹² where $\eta=0.042\pm 0.006$ and another in an ionic mixture¹³ where $\eta=0.030\pm 0.002$. One additional light scattering investigation has been reported for a liquid–liquid mixture¹⁴ where $\eta=0.045\pm 0.011$, but with no multiple scattering correction.¹⁵ The thesis of Shanks¹⁶ reports $\eta=0.033\pm 0.023$ from light scattering measurements on isobutyric acid and water when using multiple scattering corrections to second order. The recent experimental values for η vary from 0.038 to 0.045 with errors from 10% to 25%. We previously determined consistency with Ferrell’s prediction for the turbidity from preliminary data¹¹ on a near-critical, density-matched, liquid–liquid mixture methanol–cyclohexane when within microKelvins of the critical point. This paper presents the final data taken on that system, but closer to the critical composition and with better precision and reproducibility.

II. THEORY

Green and Fisher¹⁷ first proposed the critical correlation-correction exponent η to describe how the correlation function behaves asymptotically close to T_c . This exponent is fundamental to the theory of second-order phase transitions. Recent field theoretic analysis and partial differential approximates give the theoretical values for γ , ν , and η shown in Table I, where the scaling relation $\gamma=(2-\eta)\nu$ is used. Ferrell and Bhattacharjee¹⁸ argued that η can be determined by a sum rule with a value of $\eta\approx 0.04$.

In 1991, Ferrell¹⁹ developed the theory that would allow turbidity measurements to be used to determine η , a parameter which appears explicitly in his formulation. The turbidity is related to critical phenomena by assuming Ornstein–Zernike ($\eta=0$) scattering²⁰ when in the vicinity of, but not too close to, the critical point and a modified¹⁹ Fisher–Burford²¹ form ($\eta\neq 0$) when very close to critical. Having $\eta\neq 0$ is expected to result in lower turbidity values at small reduced temperatures (close to the critical point), but identical turbidity values as O–Z when at large reduced temperatures. With few exceptions,^{11,22} previous turbidity experiments^{6–9,11,23,24} have neglected η because data could not be taken sufficiently close to the critical point to warrant inclusion. The principal advantage of measuring the turbidity

is that multiple scattering has little effect on the measured transmitted beam because once the light is scattered out of the beam, it has a negligible probability of entering the detector.

Ornstein–Zernike scattering holds when in the vicinity of the critical point ($t>10^{-5}$) and assumes that the critical exponent η is zero and thus that $\gamma=2\nu$. The turbidity can be developed by integrating the light scattered out of the incident beam to give²⁰

$$\tau = \tau_0 t^{-\gamma} \left\{ \frac{2a^2 + 2a + 1}{a^3} \ln(1 + 2a) - \frac{2(1 + a)}{a^2} \right\} \quad \text{for } \eta=0, \quad t > 10^{-5}, \quad (2a)$$

or

$$\tau = \frac{\tau_0}{k_0^2 \xi_0^2} \left\{ \left(1 + \frac{1}{a} + \frac{1}{2a^2} \right) \ln(1 + 2a) - \left(1 + \frac{1}{a} \right) \right\}, \quad (2b)$$

where $a=2k_0^2\xi^2$, $k_0=2\pi n/\lambda_0$, n is the refractive index of the mixture, λ_0 is the vacuum wavelength of the light, and τ_0 is a quantity dependent on the system. The ξ_0 dependence enters in a complicated fashion through a . Even though Eq. (2a) is derived using $\eta=0$, it has been successfully used by experimentalists to describe turbidity data using the values of γ and ν from Table I when $\eta\neq 0$. Because of this, Ferrell²⁵ points out that it is more appropriate to use Eq. (2b) where the exponent γ does not appear since $t^{-\gamma}$ cancels $t^{-2\nu}$ within one of the a terms in the denominator. There is no distinction between Eqs. (2a) and (2b) if γ is 1.26, but a significant difference if γ is 1.237 in Eq. (2b). Equation (2a) will be referred to as the Puglielli–Ford (P–F) equation²⁰ where $\gamma=1.237$, while (2b) as Ornstein–Zernike (O–Z) where implicitly $\gamma=2\nu=1.26$. When very close to the critical temperature ($t<10^{-5}$ or $a>80$), then O–Z has a $\ln(t)$ dependence while P–F has an additional $t^{\eta\nu}$. Thus, the turbidity predicted by O–Z is much larger than that from P–F. This is a region in temperature where O–Z is known to be inadequate, and Ferrell¹⁹ has developed an expression for the turbidity that includes the critical exponent η . As we will see, Ferrell’s prediction, as well as the experimental data, fall between the predictions of O–Z and P–F.

When very close to the critical point, Ferrell¹⁹ uses a modified Fisher–Burford²¹ form of the critical point’s spatial correlation function to obtain [his Eq. (25)]

$$\tau = \frac{\tau_0}{k_0^2 \xi_0^2} \left\{ L - 1 - \frac{\eta}{4} L^2 + 8.37 \eta \right\} \quad t < 10^{-5}, \quad (3)$$

where $L=\ln(2a)$. It is important to note that the “normalization” prefactor to the bracketed expression in Eq. (3) is corrected from the one used in our earlier publication.¹¹ In his publication, Ferrell leaves the prefactor out and states that the turbidity is normalized to “the scattering intensity at its value in the backward scattering direction.”¹⁹ Until informed by Ferrell,²⁵ we had not appreciated the distinction between P–F and O–Z represented by Eq. (2) and that Ferrell’s prediction extends O–Z when the system is very close to critical.

Martin-Mayor, Pelissetto, and Vicari²⁶ did a Monte Carlo simulation of the 3D Ising model on a simple cubic lattice of length 128 and 256 and also developed an analytical expression for the turbidity when close to the critical point (their Eq. (34))

$$\tau = \frac{4\tau_0 t^{-\gamma}}{a} C_1^+ \left\{ (2a)^{\eta/2} \left(\frac{\eta^2 + 2\eta + 8}{\eta(\eta + 2)(\eta + 4)} \right) - \frac{1}{\eta} + \frac{K}{C_1^+} \right\}, \quad t < 10^{-5}, \quad (4)$$

where a is the same as in Eq. (2) or (3), $C_1^+ = 0.918$, and $K = 0.145 \pm 0.016$ is determined in the simulation when the exponents η , γ , and ν are those in the first row of Table I. They

$$\tau = 4\tau_0 t^{-\gamma} \frac{[(2b + 1)^{\eta/2} - 1][4 - 2b(\eta - 4) + b^2(\eta^2 + 2\eta + 8)] - 4\eta b(1 + b)}{b^3 \eta(2 + \eta)(4 + \eta)}, \quad (5)$$

where $b = 2a/(2 - \eta)$. This expression gives a larger turbidity than Ferrell's equation¹⁹ or the Martin-Mayor equation,²⁶ but a smaller turbidity than O-Z. We can compare the five expressions we have for the turbidity in Fig. 1 when $\gamma = 1.237$ and $\eta = 0.036$.

Because the constant τ_0 is strongly coupled to the value of the critical exponent γ , the expressions [Eqs. (2a), (4), (5)] with an explicit $t^{-\gamma} = t^{-1.237}$ in front require a larger τ_0 than Eq. (2b) or (3), which has an implicit $t^{-2\nu} = t^{-1.26}$. The difference is due to the $t^{-\gamma}/a$ in Eq. (4) that forces a different value for τ_0 (see the Appendix). Figure 1 shows the turbidity as a function of reduced temperature t for the different functions and illustrates how O-Z and P-F, when extended close to the critical point, bracket the other three predictions. In

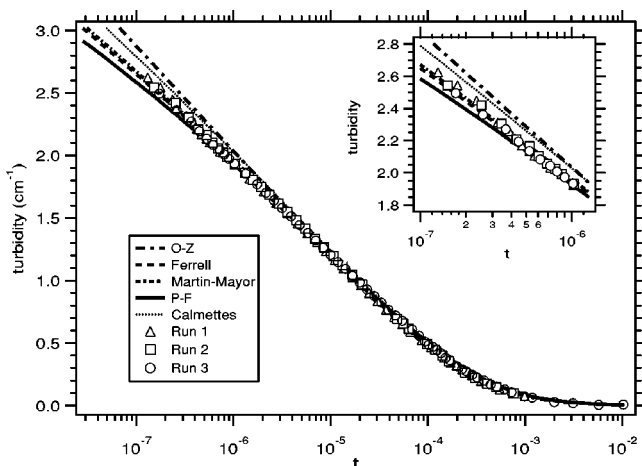


FIG. 1. The three runs of turbidity data as a function of reduced temperature t are shown with the theoretical predictions using the parameter values from fit 4 in Table III (see the text for details) and the exponents from the first row of Table I. O-Z is Eq. (2b), P-F is Eq. (2a), Ferrell is Eq. (3), Martin-Mayor is Eq. (4), and Calmettes is Eq. (5). The inset shows the region closest to the critical point.

found the turbidity to be larger than P-F, but consistent with Ferrell's prediction. When K is at the lower end of its range, we also find Eq. (4) to give equivalent values of the turbidity to those calculated from Eq. (3). The equivalence of the two expressions is shown in the Appendix. We make the distinction between P-F and O-Z in part to make it clear²⁷ that our prior experimental results are consistent with both Ferrell's theory¹⁹ and Martin-Mayor's equation:²⁶ the turbidity is larger than P-F but smaller than O-Z.

Finally, Calmettes *et al.*²² developed an expression for the turbidity that includes η and covers the entire range of temperatures investigated in this experiment. Martin-Mayor²⁶ corrected the definition of the correlation function by Calmettes to give

comparing the functions in this plot, we require the value of the turbidity to match at $t = 10^{-5}$ in Eqs. (2a) and (2b), with the result that τ_0 in Eq. (2a) is larger by a factor $t^{\eta\nu} \approx 1.3$. The other parameter values are from fit 4 in our last table with $\gamma = 1.237$. For Eq. (4), τ_0 is the same as in Eq. (2b), $C_1^+ = 0.918$ and $K = 0.129$.

Figure 2 compares the ratio of the different turbidity expressions to the prediction from P-F. The same parameter values are used as in Fig. 1, but the ratio illustrates the differences among the predictions in comparison to our experimental data. It is important to note that the ratio is quite sensitive to the choice of exponent values and normalizing constants. Still, it provides a useful way to visualize the intercomparison among the theories and our data.

III. EXPERIMENT

In this experiment, we measure the turbidity in a liquid-liquid mixture when very near the critical point. The system

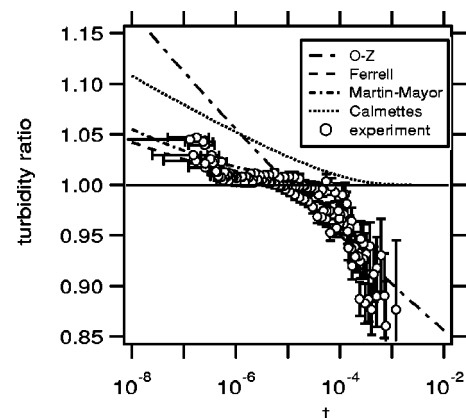


FIG. 2. The ratio of the turbidity from each of the theoretical expressions divided by the turbidity predicted by P-F. The parameter values are the same as in Fig. 1. The three runs of turbidity data are combined and also divided by the turbidity calculated by P-F.

we investigate is the nearly density-matched mixture of methanol and cyclohexane at its critical composition. We are able to measure the turbidity over a wide range of reduced temperatures that allows us to explore both the range of most turbidity experiments ($10^{-5} < t < 10^{-2}$) as well as the region very close to the critical point ($10^{-7} < t < 10^{-5}$). No attempt is made to look for crossover⁴ behavior when further from the critical point ($t > 10^{-2}$) due to the small amount of light scattering in this system when far from critical.

This system has been extensively studied, which is one of the reasons for choosing it. The coexistence curve has been measured²⁸ along with the effects of impurities²⁹ on the location of the critical point. The turbidity has been measured over a region of reduced temperature ($t > 10^{-7}$) by several groups.^{23,24,30} The effect of multiple scattering is known,³¹ along with the heat capacity.³²

The critical point depends on the purity of the system. The methanol and cyclohexane system is very sensitive to water impurities,²⁹ but any impurity will cause the critical temperature and critical composition to change systematically.³³ By measuring the critical temperature, the critical composition can be determined: for critical temperatures around 319.3 K, the critical concentration is 30.0% by mass methanol.²⁹

The fluids we used were HPLC grade methanol (Aldrich 99.93% pure) and cyclohexane (Fluka 99.8% pure) used without further purification. The total water present is stated to be less than 0.02%. A glove box with a dry nitrogen atmosphere was used when filling the cell with the fluids at a concentration of $29.9\% \pm 0.7\%$ by mass methanol. The densities of the pure components are matched to 1.6% and thus experience negligible gravitational stratification. We observed a (flat) meniscus to form in the center of the cell when just below (< 1 mK) the critical temperature. A meniscus that divides the two phases into equal volumes at the critical point indicates that the fluids are at the critical concentration.

An optical cell of our own design seals the fluids between two optical glass flats within a copper cylinder using Kalrez o-rings. The distance between the windows, or the path length of the fluids, was measured using a traveling microscope to be 1.100 ± 0.002 cm. The thermostat which surrounds the cell is made of three nested copper cylinders, each held in place by nylon spacers. The thermostat and temperature-controlling electronics are described in a previous publication.¹¹ The temperatures of the stages and the light intensities are recorded every program cycle (4 min). We can control the temperature of the cell to within $10 \mu\text{K}$ for several hours at temperatures near the system's critical temperature of 319.3 K.

The optical layout for this experiment was also described previously.¹¹ We now use an intensity stabilized (Melles Griot 05 STP 901) HeNe laser (wavelength 632.8 nm) and use a Stanford Research System SR830 lock-in amplifier tuned to an optical chopper to monitor the transmitted intensity through the fluids. A separate lock-in monitors the portion of the laser beam directed around the fluids by a beam splitter. The intensity of the beam passing through the fluids is small since the beam first passes through a beam expander/spatial filter and then a 1 mm aperture. As a result, the laser

beam does not cause any measurable local heating of the fluids. The transmitted light intensity was detected by a photodiode with an acceptance angle of 0.3° .

An average of the ratio of light intensity through the fluids "I" to that around the fluids "I₀" is used to calculate the raw turbidity from Eq. (1). Since the beam splitter does not divide the light evenly, and since the windows on the stages of the thermostat reflect some of the incident light, the raw turbidity will be offset by a background turbidity, an additive constant that represents the beam splitter and reflection effects. The background turbidity is determined experimentally for each data run with an error of 0.005 cm^{-1} by measuring the raw turbidity when the fluids are several degrees above the critical temperature, where the fluids are clear and the actual turbidity is effectively zero. The absolute turbidity presented below has the appropriate background turbidity subtracted from the raw turbidity.

The location of the critical temperature is determined within $30 \mu\text{K}$ ($t = 9 \times 10^{-8}$) by a sharp drop in the transmitted light intensity. We collected turbidity data for three runs that approached the critical temperature closely; in all, 136 data points with 66 points within 3 mK of the critical temperature. Each data run took many days and started several degrees above the critical temperature and then lowered in steps down to the critical point. All the data were consistent with each other and with the preliminary data we reported earlier. As with our earlier data, the critical temperature drifted upward approximately linearly in time at 0.45 mK/h . This was attributed to water contamination²⁹ leaching from the cell walls or glass window surfaces, even though we baked the cell parts in a vacuum oven before assembly. We used the critical temperature drift to slowly bring the cell to the critical point by fixing the temperature after the last step (about 10 mK above critical) and then continuously collecting data while the system went through the critical point. Once the transmitted intensity dropped sharply, we could observe a meniscus form in the center of the cell indicating the phase transition at the critical composition.

The three sets of absolute turbidity data are tabulated in Table II and shown in Fig. 1, which illustrates the good reproducibility. The reduced temperature $t = (T - T_c)/T_c$ takes into account the drift in the critical temperature using the time when each data point was taken. The error bars are omitted for clarity, but on this plot would show only for the points close to critical (small reduced temperature t) where we assigned an error of 1.2×10^{-7} plus an error in the critical temperature drift of $20 \mu\text{K/h}$. The error in the measured turbidity values was 0.005 cm^{-1} and due principally to the uncertainty in the background turbidity. Before doing a weighted fit to the theoretical expressions, the errors in reduced temperature were propagated into the turbidity error.

IV. ANALYSIS

In comparing our data to the five distinct theoretical expressions, we use the range of temperatures over which the expressions are valid. In this experiment, the wavelength of the laser light is 632.8 nm and the refractive index of the mixture²⁸ at the critical point is 1.380, which gives the wave number $k_0 = 0.01370 \text{ nm}^{-1}$. As described above, we use ex-

TABLE II. Our experimental data for the turbidity τ as a function of reduced temperature t . $\delta\tau$ is the total propagated error in the turbidity and represents the uncertainty in the raw intensity measurements as well as in the reduced temperature.

t	τ (cm ⁻¹)	$\delta\tau$ (cm ⁻¹)	t	τ (cm ⁻¹)	$\delta\tau$ (cm ⁻¹)
Run 1					
9.87E-04	0.075	0.005	3.58E-06	1.548	0.027
7.42E-04	0.097	0.005	2.90E-06	1.615	0.029
5.48E-04	0.130	0.0052	2.34E-06	1.686	0.032
3.53E-04	0.198	0.0057	1.92E-06	1.747	0.036
2.83E-04	0.244	0.0062	1.58E-06	1.804	0.04
2.46E-04	0.270	0.0067	1.31E-06	1.860	0.045
2.24E-04	0.289	0.0071	1.03E-06	1.932	0.052
1.96E-04	0.319	0.0074	8.61E-07	1.990	0.059
1.71E-04	0.341	0.008	7.82E-07	2.024	0.063
1.46E-04	0.383	0.0088	6.90E-07	2.058	0.069
1.18E-04	0.444	0.0092	6.05E-07	2.103	0.076
1.08E-04	0.468	0.011	5.29E-07	2.165	0.084
9.87E-05	0.489	0.011	4.34E-07	2.208	0.099
8.62E-05	0.522	0.012	3.45E-07	2.305	0.12
6.59E-05	0.591	0.014	2.53E-07	2.420	0.16
5.43E-05	0.653	0.014	1.52E-07	2.543	0.24
4.48E-05	0.710	0.015	Run 3		
3.69E-05	0.767	0.015	1.03E-02	0.009	0.005
3.03E-05	0.834	0.016	5.73E-03	0.006	0.005
2.48E-05	0.900	0.016	3.11E-03	0.019	0.005
2.04E-05	0.964	0.017	2.00E-03	0.028	0.005
1.67E-05	1.028	0.018	1.19E-03	0.064	0.005
1.36E-05	1.095	0.018	9.79E-04	0.074	0.005
1.10E-05	1.165	0.019	7.22E-04	0.107	0.0051
8.97E-06	1.235	0.02	6.16E-04	0.129	0.0052
7.23E-06	1.307	0.021	5.09E-04	0.151	0.0053
5.79E-06	1.381	0.022	4.43E-04	0.169	0.0055
4.58E-06	1.458	0.024	3.77E-04	0.199	0.0057
3.55E-06	1.540	0.026	3.22E-04	0.223	0.006
2.75E-06	1.622	0.029	2.86E-04	0.247	0.0063
2.05E-06	1.712	0.034	2.50E-04	0.273	0.0067
1.47E-06	1.815	0.041	2.24E-04	0.290	0.0069
1.03E-06	1.925	0.052	1.98E-04	0.314	0.0076
7.24E-07	2.032	0.066	1.68E-04	0.362	0.0084
5.68E-07	2.105	0.08	1.52E-04	0.382	0.0089
5.27E-07	2.134	0.085	1.36E-04	0.418	0.0095
4.69E-07	2.170	0.093	1.24E-04	0.444	0.0099
4.21E-07	2.212	0.1	1.12E-04	0.469	0.01
3.88E-07	2.258	0.11	1.02E-04	0.486	0.011
3.26E-07	2.314	0.13	9.32E-05	0.510	0.011
2.55E-07	2.375	0.16	8.11E-05	0.557	0.012
2.36E-07	2.449	0.16	6.89E-05	0.606	0.013
1.77E-07	2.543	0.21	5.45E-05	0.678	0.015
1.31E-07	2.624	0.28	4.62E-05	0.720	0.015
Run 2					
7.64E-04	0.098	0.0051	3.92E-05	0.766	0.016
5.06E-04	0.148	0.0053	3.31E-05	0.823	0.016
4.05E-04	0.175	0.0054	2.80E-05	0.875	0.017
3.05E-04	0.220	0.0058	2.36E-05	0.928	0.017
2.40E-04	0.264	0.0063	1.99E-05	0.984	0.018
1.65E-04	0.355	0.0076	1.68E-05	1.038	0.018
1.40E-04	0.399	0.0083	1.41E-05	1.093	0.019
1.19E-04	0.447	0.01	1.19E-05	1.147	0.019
9.75E-05	0.495	0.01	9.95E-06	1.206	0.02
6.37E-05	0.613	0.011	8.37E-06	1.262	0.021
5.53E-05	0.654	0.011	7.01E-06	1.319	0.022
4.83E-05	0.693	0.011	5.83E-06	1.380	0.023
2.11E-05	0.966	0.017	4.79E-06	1.445	0.024
1.67E-05	1.047	0.018	3.89E-06	1.514	0.026
1.33E-05	1.123	0.019	3.16E-06	1.581	0.028
1.06E-05	1.195	0.02	2.61E-06	1.641	0.031
8.57E-06	1.265	0.02	2.15E-06	1.702	0.034
6.90E-06	1.334	0.021	1.75E-06	1.769	0.038
5.49E-06	1.414	0.023	1.34E-06	1.854	0.045
4.42E-06	1.481	0.025	1.02E-06	1.934	0.053
			8.99E-07	1.973	0.058

TABLE II. (Continued.)

t	τ (cm ⁻¹)	$\delta\tau$ (cm ⁻¹)
8.02E-07	2.008	0.063
7.21E-07	2.044	0.068
6.20E-07	2.083	0.077
5.25E-07	2.135	0.087
4.46E-07	2.193	0.099
3.67E-07	2.270	0.12
2.60E-07	2.361	0.16
1.72E-07	2.495	0.22

perimental measurements to determine the critical temperature and the background turbidity, which are not varied in the fits to the theories. We use a weighted least-squares fit³⁴ performed by a commercial package (IGOR PRO 4.07) with the parameter errors given as 1 standard deviation. The parameters and their errors are given in Table III for the different expressions.

The P-F and O-Z functions given in Eq. (2) are valid in a region where the critical exponent η does not contribute to the turbidity. This corresponds to reduced temperatures $t > 10^{-5}$. O-Z requires $\eta=0$ by forcing $\gamma=2\nu=1.26$, while P-F uses $\nu=0.63$ and $\gamma=1.237$. When we fit these functions to our data, we get parameter values of ξ_0 from 0.29 to 0.32 nm and τ_0 from 6.55 to 5.8×10^{-6} cm⁻¹ that are shown as fits 1-3 in Table III. The value of τ_0 is larger for P-F than O-Z by the factor $t^{\eta\nu}$; approximately 1.1 over this region of reduced temperatures (see fits 1 and 3 in Table III). When the critical exponents are allowed to vary using P-F, then the exponent values γ and ν are consistent with an Ising model, but not very well determined (see fit 2 in Table III). This is typical of turbidity data fit by P-F over this range of reduced temperatures.

When Ferrell's extension [Eq. (3)] of O-Z is used when the reduced temperature t is smaller than 10^{-5} and O-Z [Eq. (2b)] is used when $t > 10^{-5}$, then the data are well described. If the critical exponents ν and η are fixed at their theoretical values (fit 4 in Table III) then the values of ξ_0 and τ_0 are larger than when O-Z is used alone (fit 3). However, in fit 6 when τ_0 is fixed at the value determined by O-Z alone (fit 3), then the data are better fit (as reflected in the smaller

reduced chi square³⁴), the exponents are quite consistent with the theoretical values, and ξ_0 is consistent with fit 3 and with values published earlier. Since Eq. (4) gives equivalent values for the turbidity as Eq. (3) when the same parameters are used, we did not fit the data by the expression proposed by Martin-Mayor.²⁶

Finally, we attempted to fit the data using the turbidity expression Eq. (5) proposed by Calmettes *et al.*²² and corrected by Martin-Mayor.²⁶ Even though the exponents were fixed at the theoretical values, this function did not fit the data nearly as well (see fit 7 in Table III) as the combination of Ferrell's and O-Z.

Our data are compared to the theoretical expressions in Figs. 1 and 2. The theory lines use the parameters from fit 4 in Table III as described above. Figure 1 shows that the data are quite consistent with the predictions by Ferrell or Martin-Mayor and lie below O-Z but above P-F. Figure 2 highlights the differences by dividing the different predicted turbidities by the value predicted by P-F.²⁶ The data points in Fig. 2 are divided by the value calculated by the P-F expression at each reduced temperature. We omit the error bars in Fig. 1 for clarity, but include them in Fig. 2. At larger reduced temperatures, the error in the turbidity ratio for the data points in Fig. 2 becomes quite large because the turbidity values are so small.

V. CONCLUSION AND DISCUSSION

Our group and others have previously measured the turbidity of methanol and cyclohexane near its critical point. Our present turbidity data are consistent with those prior published data, but we are able to better determine the correlation length amplitude because of the larger number of data very near the critical temperature. Houessou *et al.*²⁴ noted that "close to T_c it is the amplitude ξ_0 which can be measured;" however, they obtained only six data points within $t < 10^{-4}$ which resulted in relatively large errors in their determination of $\xi_0 = 0.324 \pm 0.023$ nm using P-F. About the same time we²³ had also measured the turbidity and used P-F with the critical exponents fixed (but $\gamma=1.241$) to analyze data over the region $10^{-5} < t < 10^{-2}$ and found $\xi_0 = 0.324 \pm 0.006$ nm. Prior to either of those

TABLE III. Parameter values resulting from a weighted fit of the different theoretical expressions to our turbidity data. P-F is Eq. (2a), O-Z is Eq. (2b), Ferrell extends O-Z in Eq. (3), and Calmettes is Eq. (5). The Martin-Mayor expression in Eq. (4) gives results equivalent to Ferrell's equation. The region in reduced temperature is either "far" when $10^{-5} < t < 10^{-2}$ or "all" when $10^{-7} < t < 10^{-2}$. Parameters without errors are fixed in the fit, the errors are one standard deviation estimates, and χ^2/N is the reduced chi-square.

Fit #	Region	Function	$10^6 \tau_0$ (cm ⁻¹)	ξ_0 (nm)	ν	γ	η	χ^2/N
1	Far	P-F	6.55±0.08	0.294±0.003	0.63	1.237	...	0.66
2	Far	P-F	5.6±3.1	0.24 ±0.02	0.65±0.03	1.25±0.08	...	0.59
3	Far	O-Z	5.80±0.07	0.320±0.003	0.63	0.77
4	All	O-Z & Ferrell	6.01±0.05	0.332±0.002	0.63	...	0.036	0.56
5	All	O-Z & Ferrell	5.99±0.06	0.331±0.002	0.63	...	0.042±0.005	0.55
6	All	O-Z & Ferrell	5.8	0.327±0.001	0.632±0.002	...	0.040±0.005	0.54
7	All	Calmettes	6.93±0.06	0.314±0.002	0.63	1.237	0.036	0.67

measurements, Kopelman *et al.*³⁰ measured the turbidity in a very thin (0.02 cm) sample and collected data as close to the critical temperature as we report here. However, they could measure an effect only close to T_c ($t < 10^{-4}$) and with large random errors in the turbidity (0.1 cm^{-1}) that, when analyzed using P–F, resulted in a large uncertainty in the correlation length $\xi_0 = 0.39 \pm 0.10 \text{ nm}$. Their data scatters around our present results and confirms that multiple scattering does not affect our data. Our result for $\xi_0 = 0.330 \pm 0.003 \text{ nm}$ is within the error of all of these determinations and is better determined because of the large number of data close to T_c (over 90 points within $t < 10^{-4}$).

The turbidity of the liquid–liquid mixture methanol and cyclohexane has been measured very near its upper critical consolute point over several decades in reduced temperature. Our experimental turbidity data in the region very close to the critical point are smaller than predicted by O–Z but larger than P–F. The data are consistent with both Ferrell’s expression and with the one by Martin-Mayor *et al.* The limit in our data is not the temperature control or the resolution in measuring light intensity, but the drift in the critical temperature. Even though this drift was uniform, the uncertainty introduced by it limited our knowledge of the critical exponents and amplitudes. Nevertheless, we could determine the values of those exponents and amplitudes by fitting the data over the entire range of five decades in reduced temperature.

The O–Z and P–F expressions could equally well describe the data over the region where they apply ($t > 10^{-5}$), which indicates that these turbidity data could not distinguish between $\gamma = 1.237$ and 1.26 , which is typical for turbidity data. Ferrell’s extension of O–Z when close to the critical point could be used with O–Z at higher temperatures to describe the data well and determine the critical exponents $\nu = 0.632 \pm 0.002$ and $\eta = 0.041 \pm 0.005$, consistent with theoretical predictions, and the amplitudes $\xi_0 = 0.330 \pm 0.003 \text{ nm}$ and $\tau_0 = (5.9 \pm 0.1) \times 10^{-6} \text{ cm}^{-1}$ (errors are 1 standard deviation estimates). Ferrell’s expression and the one by Martin-Mayor *et al.* are equivalent over the region close to the critical point. The expression by Calmettes *et al.* (as corrected by Martin-Mayor *et al.*) could be used over the entire range of our data, but did not fit the data as well as Ferrell’s and O–Z. It has already been noted²⁶ that the expression by Calmettes, even when corrected, gives turbidity values that are too large, and we find this to also be the case when trying to fit our data.

ACKNOWLEDGMENTS

Acknowledgment is made to NASA, Grant NAG8-1433 for support of this research. A.L. acknowledges summer support from an NSF-REU grant. D.T.J. thanks the Henry Luce III Fund for Distinguished Scholarship as administered by The College for release time. We appreciate the helpful discussions with Richard Ferrell.

APPENDIX: CONSISTENCY OF FERRELL AND MARTIN-MAYER *ET AL*

The expression for the turbidity asymptotically close to the critical point developed by Ferrell [Eq. (3)] looks quite different from a corresponding expression developed by Martin-Mayor *et al.* [Eq. (4)]. Although they develop a similar expression to Ferrell’s in their paper [their Eq. (38)], they pick a “normalizing constant,” $g(2Q_0)$, that has a temperature dependence in part because of the confusion alluded to earlier in this paper about the prefactor to Ferrell’s expression. In this Appendix we show that the Martin-Mayor *et al.* result [Eq. (4)] can be rewritten to correspond to Ferrell’s result [Eq. (3)] in the appropriate limit of small η and small reduced temperature t .

We can approximate

$$(2a)^{\eta/2} \approx 1 + \frac{\eta}{2}L + \frac{\eta^2}{8}L^2,$$

where $L \equiv \ln(2a)$ to take Eq. (4) to

$$\tau \approx \frac{2\tau_0 t^{-\gamma}}{a} C_1^+ \left\{ (L-1) + \eta \left(\frac{L^2}{4} - \frac{L}{2} + \frac{3}{4} \right) + \frac{K}{C_1^+} \right\},$$

which is the same as Eq. (37) in Ref. 26. Since $t^{-\gamma/a} = t^{\eta\nu}/(2k_0^2 \xi_0^2)$ and

$$t^{\eta\nu} \approx \left[1 - \frac{\eta}{2}L \right] \left[1 + \frac{\eta}{2} \ln(4k_0^2 \xi_0^2) \right],$$

then the previous equation reduces to

$$\tau \approx \frac{\tau_0 C}{k_0^2 \xi_0^2} \left[L - 1 - \eta \frac{L^2}{4} + \eta \left(\frac{3}{4} + \frac{K}{\eta C_1^+} \right) \right],$$

which is the same as Eq. (3) except for the constant factor $C \equiv C_1^+ (1 + (\eta/2) \ln(4k_0^2 \xi_0^2)) \approx 0.76$ for our system and the different constant multiplying η in the last term. The factor C is why the value of τ_0 needs to be larger by $1/C = 1.3$ when comparing to our experimental data. The last term is less than 1 percent of L and is at the limit of our experimental resolution for the turbidity. Thus, the equation given by Martin-Mayor *et al.* [Eq. (4)] is the same as that given by Ferrell [Eq. (3)] within our experimental resolution.

¹J. V. Sengers and J. M. H. Levelt-Sengers, *Annu. Rev. Phys. Chem.* **37**, 189 (1986); S. C. Greer and M. R. Moldover, *ibid.* **32**, 233 (1981); A. Kumar, H. R. Krishnamurthy, and E. S. R. Gopal, *Phys. Rep.* **98**, 57 (1983).

²A. Pelissetto and E. Vicari, *Phys. Rep.* **368**, 549 (2002).

³M. Campostrini, A. Pelissetto, P. Rossi, and E. Vicari, *Phys. Rev. E* **65**, 066127 (2002).

⁴R. Guida and J. Zinn-Justin, *J. Phys. A* **31**, 8103 (1998).

⁵M. E. Fisher, S.-Y. Zinn, and P. J. Upton, *Phys. Rev. B* **59**, 14533 (1999); A. J. Liu and M. E. Fisher, *Physica A* **156**, 35 (1989).

⁶A. W. Nowicki, M. Ghosh, S. M. McClellan, and D. T. Jacobs, *J. Chem. Phys.* **114**, 4625 (2001).

⁷J. Jacob, M. A. Anisimov, J. V. Sengers, V. Dechabo, I. K. Yudin, and R. W. Gammon, *Appl. Opt.* **40**, 4160 (2001).

⁸S. G. Stafford, A. C. Ploplis, and D. T. Jacobs, *Macromolecules* **23**, 470 (1990).

- ⁹S. Wiegand, M. E. Briggs, J. M. H. Levelt-Sengers, M. Kleemeier, and W. Schroer, *J. Chem. Phys.* **109**, 9038 (1998).
- ¹⁰M. E. Fisher, lecture notes presented at the "Advanced course on critical phenomena," January 1982 at Merensky Institute, University of Stellenbosch, South Africa.
- ¹¹D. T. Jacobs, S. M. Y. Lau, A. Mukherjee, and C. A. Williams, *Int. J. Thermophys.* **29**, 877 (1999).
- ¹²P. Damay, F. Leclercq, R. Magli, F. Formisano, and P. Lindner, *Phys. Rev. B* **58**, 12038 (1998).
- ¹³P. Damay, F. Leclercq, and P. Chieux, *Phys. Rev. B* **40**, 4696 (1989).
- ¹⁴O. Muller and J. Winkelmann, *Phys. Rev. E* **59**, 2026 (1999).
- ¹⁵A. E. Bailey and D. S. Cannell, *Phys. Rev. E* **50**, 4853 (1994).
- ¹⁶J. G. Shanks, "A light scattering study of static critical phenomena in binary liquid mixtures" (Ph.D. thesis, University of Maryland, 1986).
- ¹⁷M. E. Fisher, *J. Math. Phys.* **5**, 944 (1964).
- ¹⁸R. A. Ferrell and J. K. Bhattacharjee, *Phys. Rev. Lett.* **42**, 1505 (1979).
- ¹⁹R. A. Ferrell, *Physica A* **177**, 201 (1991).
- ²⁰V. G. Puglielli and N. C. Ford, Jr., *Phys. Rev. Lett.* **25**, 243 (1970).
- ²¹M. E. Fisher and R. J. Burford, *Phys. Rev.* **156**, 583 (1967).
- ²²P. Calmettes, I. Lagues, and C. Laj, *Phys. Rev. Lett.* **28**, 478 (1972).
- ²³D. T. Jacobs, *Phys. Rev. A* **33**, 2605 (1986).
- ²⁴C. Houessou, P. Guenoun, R. Gastaud, F. Perrot, and D. Beysens, *Phys. Rev. A* **32**, 1818 (1985).
- ²⁵R. A. Ferrell (private communication, 2002).
- ²⁶V. Martin-Mayor, A. Pelissetto, and E. Vicari, *Phys. Rev. E* **66**, 026112 (2002).
- ²⁷The authors in Ref. 26 imply that the data in Ref. 11 are inconsistent with their simulation results.
- ²⁸D. T. Jacobs, D. J. Anthony, R. C. Mockler, and W. J. O'Sullivan, *Chem. Phys.* **20**, 219 (1977).
- ²⁹J. L. Tveekrem and D. T. Jacobs, *Phys. Rev. A* **27**, 2773 (1983).
- ³⁰R. B. Kopelman, R. W. Gammon, and M. R. Moldover, *Phys. Rev. A* **29**, 2048 (1984).
- ³¹C. M. Sorensen, R. C. Mockler, and W. J. O'Sullivan, *Phys. Rev. A* **16**, 365 (1977).
- ³²M. A. Anisimov, *Critical Phenomena in Liquids and Liquid Crystals* (Gordon & Breach, Philadelphia, 1991).
- ³³D. T. Jacobs, *J. Chem. Phys.* **91**, 560 (1989).
- ³⁴P. R. Bevington, *Data Reduction and Error Analysis for the Physical Sciences* (McGraw-Hill, New York, 1969).